Placement of SVCs and Selection of Stabilizing Signals in Power Systems

Malihe M. Farsangi, Hossein Nezamabadi-pour, Yong-Hua Song, *Senior Member, IEEE*, and Kwang Y. Lee, *Fellow, IEEE*

***Abstract*—This paper presents a method to seek the optimal location of several static Var compensators (SVCs) in a power system based on their primary function. Taking advantages of the flexible ac transmission system (FACTS) devices depends largely on how these devices are placed in the power system, namely, on their location and size. In addition to their primary function, the supplementary damping control action can be also added, and how to utilize their control capabilities effectively as stabilizing aids is becoming very important. In this paper, power system stability is used as an index for optimal allocation of the controllers. First, several SVCs are placed optimally based on modal analysis and genetic algorithm in a power system. After placing the SVCs based on their primary functions, the most appropriate input signal for supplementary controller is also selected. The frequency response characteristics of the system for all located SVCs are determined in selecting the best input signals.**

***Index Terms*—Genetic algorithm, inter-area oscillation, modal analysis, optimal placement, stabilizing signal, static Var compensator (SVC), voltage stability.**

I. Introduction

TODAY, most power systems are operating near their steady-state stability limits, which may result in voltage instability. Flexible ac transmission system (FACTS) devices are good choices to improve the stability of power systems. Many studies have been carried out on the use of FACTS devices for voltage and angle stability problems. Taking advantages of the FACTS devices depends largely on how these devices are placed in the power system, namely, on their location and size. In a practical power system, allocation of these devices depends on a comprehensive analysis of steady-state stability, transient stability, small signal stability, and voltage stability. Moreover, other practical factors such as cost and installation conditions also need to be considered. In the literature, a tool has been reported based on the determination of critical modes, which is known as modal analysis [1], [14], [22]. Modal analysis has been used to locate static Var compensator (SVC) and other shunt compensators to avoid voltage instability. The siting of many controllable power system devices, such as HVDC Links and FACTS devices, are based on the issues unrelated to the damping of oscillations in the system. For instance, an SVC improves transmission system voltage, thereby enhancing the maximum power transfer limit; static synchronous series compensator (SSSC) control reduces the transfer impedance of a long transmission line, enhancing the maximum power transfer limit. In addition to the primary function, the supplementary damping control is also added, and how to utilize their control capabilities effectively as stabilizing aids is becoming very important.

Over the last decades, there has been a growing interest in algorithms inspired by observing natural phenomenon. It has been shown that these algorithms are good alternatives as tools in solving complex computational problems. Various heuristic approaches have been adopted in research, including genetic algorithm [2]–[6], tabu search [7], simulated annealing [8], etc. Cai *et al.* [2] used a genetic algorithm to determine the best location of a given set of FACTS devices in a deregulated electricity market. In [3] and [4], the optimal locations of FACTS devices are obtained for Var planning. Gerbex *et al.* [5] used a genetic algorithm to place different types of FACTS devices in a power system. In their study, the number of devices to install is assigned before optimization. In [6], a methodology is carried out using a genetic algorithm to find the optimal number and location of thyristor-controlled phase shifters in a power system.

In this paper, power system stability is used as an index for optimal allocation of SVCs. For this, several SVCs are placed in a power system based on their primary function, which is the voltage stability. To locate SVCs based on the voltage stability, two methods are used: modal analysis and genetic algorithm. It will be shown that the results obtained by the two methods are similar. However, with the modal analysis, the SVCs cannot be placed in the power system optimally since the optimal sizes of SVCs are unknown. Because of this problem, the sizes of the SVCs are obtained by a genetic algorithm. To take advantages of FACTS devices, the ability of the SVCs in damping the inter-area oscillations (in the frequency range of 0.1–2 Hz) is investigated, where selecting the proper signals is playing an important role.

The work presented in [10] is a modified method of [9] to select the supplementary input signal for STATic synchronous COMpensator (STATCOM). In this paper, the proposed method is modified further. A comprehensive review is done in [9] showing how other researches answer the question of which

Manuscript received May 11, 2006; revised December 28, 2006. Paper no. TPWRS-00283-2006.

M. M. Farsangi and H. Nezamabadi-pour are with the Department of Electrical Engineering, Kerman University, 76175-133 Kerman, Iran (e-mail: mmaghfoori@mail.uk.ac.ir; nezam@mail.uk.ac.ir).

Y.-H. Song is with the Liverpool University, Liverpool L69 3GJ, U.K. (e-mail: yong-hua.song@liverpool.ac.uk).

K. Y. Lee is with the Department of Electrical and Computer Engineering, The Pennsylvania State University, University Park, PA 16802 USA, and also with Baylor University, Waco, TX 76798 USA (e-mail: kwanglee@psu.edu; Kwang_Y_Lee@baylor.edu).

Digital Object Identifier 10.1109/TPWRS.2007.901285

locations and feedback signals could result in the power system stabilizers (PSSs) and the FACTS devices having the maximum effect on the system damping. However, a brief overview is given in this paper to provide a proper background.

A detailed study on the use of an SVC for damping system oscillation is carried out in [11]. Having considered several factors including observability and controllability, it was concluded that the most suitable supplementary input signal for an SVC for damping improvement is the locally measured transmission line-current magnitude. This signal is also used in the study system carried out in [12] and [13]. Other studies, however, select locally measured active power [14], [15] or generator angular speed [16]–[18] as a supplementary input signal.

Static interaction measures derived from decentralized control theory such as the relative gain array (RGA) and controllability and observability have been applied in determining both the best location and the best input signals for multiple FACTS [19]. Several papers also deal with the combined application of controllability and observability using the singular value analysis [20], [21].

The proposed method by the authors in [9] used the minimum singular values (MSV), the right-half plane zeros (RHP-zeros), the relative gain array (RGA), and the Hankel singular values (HSV) as indicators to find stabilizing signals in single-input single-output (SISO) and multi-input multi-output (MIMO) systems. In the SISO system with one FACTS device, we use only the existence of RHP-zeros as the indicator of limiting the performance of the closed-loop system and the HSV as the indicator of controllability-observaility. On the other hand, the MSV and the RGA are useful indicators to quantify the degree of directionality and the level of interaction in the MIMO systems. In the MIMO system, using multiple FACTS devices, all four indicators are utilized.

The above-mentioned method has been modified in [10] as follows.

1) The candidates for the supplementary input signal for the STATCOM are chosen from a wide range, including global and local signals. Usually the most preferred auxiliary input signal for the STATCOM or SVC for damping improvement is the locally measured transmission line-current magnitude or line-power. However, it is shown in this paper that the locally measured signal is not necessarily the best choice.
2) While the observability and controllability of the candidates is checked using the HSV, the compared candidates should be of the same type, for example, power with power, or current with current. For the selected candidate after checking the HSV, the existence of RHP-zeros will be checked. If more than one FACTS are placed in the power system, the RGA and MSV will be checked.
3) Making the decision on the selection of final supplementary input signal has been done based on pre-fault and post-fault conditions.

In this paper, another modification is done as follows.

The RGA-number is calculated over frequency. The reason is that to avoid instability caused by interactions between different controllers, it is preferred to pair those inputs and outputs corresponding to an RGA-number close to zero.

II. Placement of SVC and Selection of Stabilizing Signals

Voltage stability is the ability of a power system to maintain acceptable voltages at all system buses under normal operation as well as following a disturbance [23]. Voltage stability can be categorized as the *large-disturbance* voltage stability and the *small-disturbance* voltage stability. The large-disturbance voltage stability is the ability of the system to control the voltage after being subjected to a large disturbance such as system faults as well as loss of load or generation. The small signal voltage stability is the ability of the system to control voltage after being subjected to a small perturbation, such as gradual changes in loads [22], [23].

In this paper two techniques are used for analysis of voltage stability, which are briefly explained below.

A. Placement Using Critical Modes of Voltage Instability (Modal Analysis)

Modal or eigenvalue analysis involves the computation of eigenvalues and eigenvectors of the system near the point of voltage collapse in order to identify different modes through which the system could come to the voltage collapse. When the modal analysis is used, the loads are gradually increased. However, there is no need to drive the system precisely to its "nose point" where the power flow does not converge to ensure that a maximum level of stress is reached.

The main conclusion from this is that voltage collapse is actually the collapse of a modal voltage. That is, the power system cannot support a particular combination of reactive power demand [22].

B. Genetic Algorithm

Genetic algorithm (GA) has desirable characteristics as an optimization tool and offers significant advantages over traditional methods. They are inherently robust and have been shown to efficiently search the large solution space containing discrete or discontinuous parameters and nonlinear constraints, without being trapped in local minima [24].

GA may be used to solve a combinatorial optimization problem. The GA searches for a solution inside a subspace of the total search space. Thus, they are able to give a good solution of a certain problem in a reasonable computation time. The optimal solution is sought from a population of solutions using a random process. Applying to the current population the following three operators creates a new generation: reproduction, crossover, and mutation. The reproduction is a process dependant on an objective function to maximize or minimize, which depends on the problem. Since the goal of the optimization problem in this paper is to find the best location and size for a number of SVCs, a configuration for an individual in a population is defined with two parameters: the location of SVCs and their Mvar sizes.

C. Selection of Auxiliary Input Signal for SVC

Stabilizing signals for SVCs are selected based on one or more of the following stability indicators: RHP-zeros, HSV, RGA, and MSV [9]. These indicators are summarized briefly in this section.

1) Right-Half Plane Zeroes (RHP-Zeros): The right-half plane zeros limit the achievable performance of a feedback loop [25], [26]. Also, from the root locus analysis, it can be seen that the locations of zeros are not changed by the feedback, but the pole locations are changed by the feedback. As the feedback gain increases, the closed-loop poles move from the open-loop poles to the open-loop zeros. Therefore, if some zeros are in the RHP, the increased gain makes the system unstable.

Thus, the selection of inputs-outputs should be carried out in such a way that the plant has a minimum number of the RHP-zeros, which are required not to lie within the closed-loop bandwidth.

2) Hankel Singular Values (HSV): Controllability and observability play an important role in selecting input-output signals. In order to specify which combination of the input and output contains more information on the system internal states, one possible approach is to evaluate observabillity and controllability indices of the system, such as HSV that reflects the joint controllability and observability of the states.

Hankel singular values can be found [9] by solving the following Lyapunov equations for the minimal realization of the state space system (A, B, C, D):

$$AP + PA^T + BB^T = 0$$
$$A^T Q + QA + C^T C = 0$$

where P and Q are the solution to the above Lyapunov equations, and

$$P = Q = diag(\sigma_1, \sigma_2, \cdots, \sigma_n)$$
$$\sigma_1 \geq \sigma_2 \geq \cdots \geq \sigma_n \geq 0$$

where the singular values σ_i (Hankel singular values) are ordered in descending order, the first singular value is the largest, and others are decreasing monotonically.

In the above realization, the value of each singular value σ_i is associated with the state x_i, and the size of the singular value is a relative measure of the contribution that the corresponding state makes to the input-output behaviors of the system. Therefore, if $\sigma_i \geq \sigma_{i+1}$, then the state x_i affects the input-output behavior more than x_{i+1} does.

In choosing input and output signals, the HSV can be calculated for each combination of inputs and outputs, and the candidate with the largest HSV shows better controllability and observability properties. It means that this candidate can give more information about system internal states [25], [26].

3) Relative Gain Array (RGA): The RGA defined by $\Lambda = G(s) \times G^{-1}(s)^T$, where $G(s)$ is a multivariable plant with m inputs and m outputs, provides useful information for the pairing of inputs and outputs. Input and output variables should be paired so that the diagonal elements of the RGA are unity as close as possible. It is desired that Λ has small elements and, for a diagonal dominance, $\Lambda - I$ to be small. These two objectives can be considered in the single objective, known as RGA-number defined as follows:

$$RGA\text{−number} = \|\Lambda - I\|_{sum} = \sum_{i=j} |1 - \lambda_{ij}| + \sum_{i \neq j} |\lambda_{ij}|. \quad (1)$$

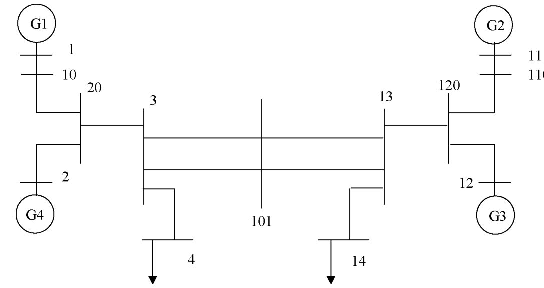

Fig. 1. Single line diagram of a two-area study system, Study System 1.

For the analysis of selection of input-output, lower RGA-number is more preferred in a control structure [24], [25].

4) Minimum Singular Value (MSV): Considering a MIMO system with transfer function G with n inputs and m outputs, G can be defined in terms of singular value decomposition as follows:

$$G = U\Sigma V^H \quad (2)$$

where $\Sigma = \begin{bmatrix} \Sigma_1 & 0 \\ 0 & 0 \end{bmatrix}$ is an $m \times n$ matrix and Σ_1 defined as

$$\Sigma_1 = \begin{bmatrix} \sigma_1 & 0 & \cdots & 0 \\ 0 & \sigma_2 & \cdots & 0 \\ \vdots & \vdots & \ddots & \vdots \\ 0 & 0 & \cdots & \sigma_k \end{bmatrix}$$

in which the nonnegative singular values $\sigma_1 \geq \sigma_2 \geq \cdots \sigma_i \geq \cdots \sigma_k \geq 0$ are placed diagonally in a descending order with $k = \min\{m, n\}$, and σ_i^2 is an eigenvalue of $G^H G$, where G^H is the complex conjugate transpose of G.

The ratio between the maximum (σ_1) and the minimum (σ_k) singular values, σ_1/σ_k, indicates the degree of directionality of the system. If this ratio is big due to small value of σ_k, it shows that the system is ill-conditioned, which indicates a large sensitivity of the system to uncertainty. To avoid ill-conditioning, it is desired that the minimum singular value σ_k be as large as possible when selecting the input-output signal [25], [26].

III. Placement of SVC in Study Systems

A. Study Systems

Two study systems are used in this paper.

1) *Study System 1: A two-area four-machine system.* This test system is illustrated in Fig. 1. The subtransient model for the generators, and the IEEE-type DC1 and DC2 excitation systems, are used for machines 1 and 4, respectively. The IEEE-type ST3 compound source rectifier exciter model is used for machine 2, and the first-order simplified model for the excitation systems is used for machine 3. PSS is placed on machines 2 and 3, and the linear models for the loads are used.
2) *Study System 2: A five-area 16-machine system.* The system shown in Fig. 2 consists of 16 machines and 68 buses for five interconnected areas. The first nine machines, G1 to G9, constitute the simple representation of Area 1. The next four machines G10 to G13, represent

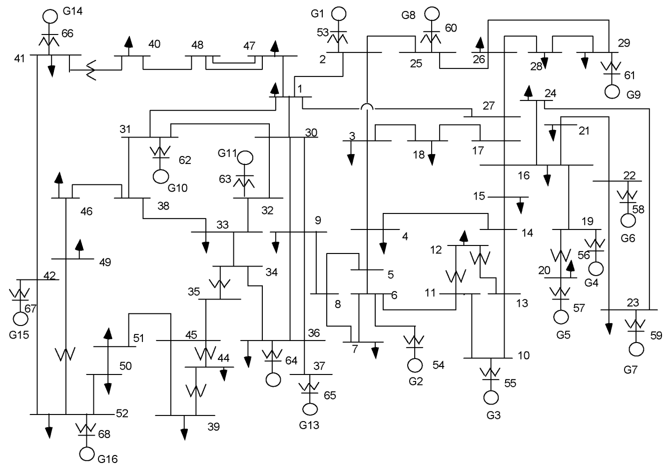

Fig. 2. Single line diagram of a five-area study system, Study System 2.

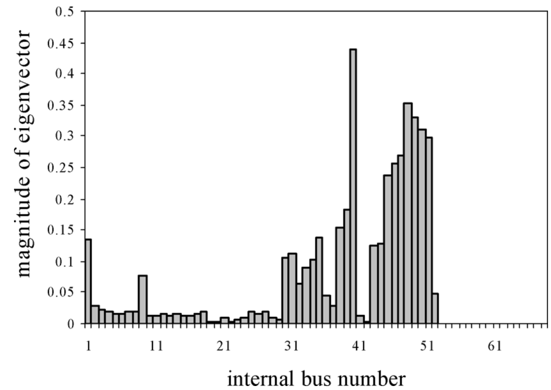

Fig. 3. Critical eigenvector and the corresponding bus number in Study System 2.

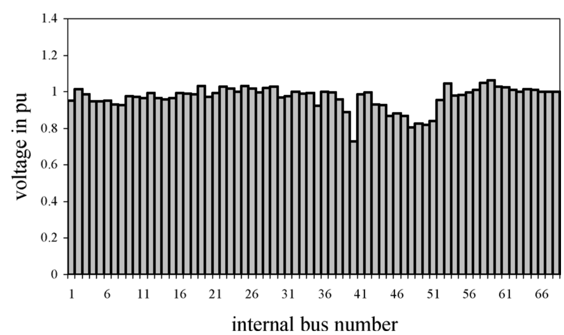

Fig. 4. Bus voltage magnitude profile when the system is heavily stressed in Study System 2.

Area 2. The last three machines, G14 to G16, are the dynamic equivalents of the three large neighboring areas interconnected to Area 2. The subtransient reactance model for the generators, the first-order simplified model for the excitation systems, and the linear models for the loads and ac network are used. A PSS is placed on machine 9.

B. Optimal Location and Sizing of SVCs

The first step is to determine suitable locations for the SVCs based on their primary function. For the Study System 1, only one SVC is located at bus 101, where voltage swings are the greatest without the SVC. In the Study System 2, genetic algorithm and modal analysis are used to optimally locate several SVCs in the power system. All loads are gradually increased to near the point of voltage collapse. The implementation of GA is as follows.

The first step in the solution of an optimization problem using GA is the encoding of the variables. The most usual approach is to represent these variables in binary as strings of 0 s and 1 s. A collection of such strings is called population.

The goal of the optimization is to find the best placement of SVCs, where the optimization is made on two parameters: their location and size. Therefore, a configuration is considered with two genes. The first gene represents the location of SVCs, and the second gene represents the size of the SVCs. For each gene, 10 bits are considered. Therefore, the length of the chromosome is 20 bits. The number of chromosomes is set to 50.

The chromosomes evolve through successive iterations, called generations. During each generation, the chromosomes are evaluated with some measure of fitness, which is calculated with the objective function. In this paper, SVCs are placed based on their primary function, which is the voltage stability. For a level of load, the following objective function is to be minimized:

$$obj = \sum abs|V_i - V_{refi}|^3 \tag{3}$$

where V_i and V_{refi} are, respectively, the actual and nominal voltage magnitudes at bus i. Equation (3) represents the sum of the voltage deviations powered to a high order, say, 3. This high order power will make the small voltage deviations very small and negligible but the large deviations relatively larger. Therefore, it will check the improvement of the voltage, only at *critical* buses resulting from the placement of the SVC.

Moving to a new generation is done based on the results obtained for the old generation. A biased roulette wheel is created with the values of the objective function evaluated for the current population. To create the next generation, new chromosomes, called offsprings, are formed using a crossover operator and a mutation operator among chromosomes selected by the roulette wheel. In this paper, the single-point crossover is applied with the crossover probability $p_c = 0.9$ and the mutation probability is selected to be $p_m = 0.005$. Also, the maximum number of iteration is set to be 70, which is the stopping criterion.

To locate SVCs in the System 2 by GA, suitable buses are selected based on 20 independent runs under different random seeds. At the first step, the obtained results by genetic algorithm show that a 145-Mvar SVC has to be placed in the system at bus 40 for voltage stability. After placing the first SVC at bus 40 and increasing the loads, the second SVC is placed at bus 49 with a Mvar size of 150.

Using modal analysis, it is also found that the weakest area in this power system is in the second area around bus 40, as illustrated in Fig. 3. Fig. 4 shows the profile of the voltage when the system is heavily stressed and reached to the point of collapse. Based on modal analysis, bus 40 is a good candidate to place

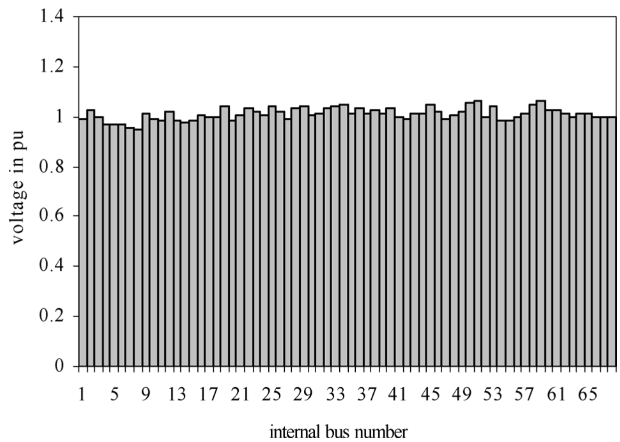

Fig. 5. Bus voltage magnitude profile of stressed system after placing a 145-Mvar SVC at bus 40 in Study System 2.

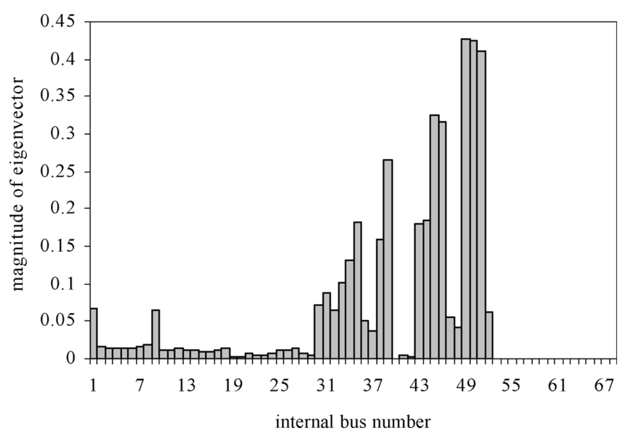

Fig. 6. Critical eigenvector and the corresponding bus number in Study System 2.

the first SVC [9]. The results obtained by the modal analysis are shown to be similar to the results obtained by the GA that specify the worst places in the areas. Using the modal analysis only, the weak point can be determined, but it cannot give any information regarding the optimal size of the SVC. However, the size is playing an important role for the SVC to be effective, and in this paper, GA is used to find the Mvar size needed for the SVC. To find the optimal compensation level, first, an SVC is placed in the Study System 2 at bus 40, and then using genetic algorithm, the Mvar size of the SVC is determined to be 145 Mvar. By optimally sizing and locating the SVC at bus 40, the power system voltage profile is improved as shown in Fig. 5. This figure shows the significant improvement of the voltages at buses 40 to 50 compared to Fig. 4.

After placing the first SVC at bus 40, once again, the loads are gradually increased. Using the modal analysis, the second-worst bus identified is bus 49 as shown in Fig. 6. Fig. 7 shows the voltage profile when the system is under stress. Again GA is used to find the optimal size of the SVC at bus 49, which yields 150 Mvar. Also, with the same procedure, the third SVC is placed at bus 50 with 150 Mvar.

By now, three SVCs are placed in the Study System 2 based on the voltage stability. For the rest of the work, the ability of the placed SVCs to damp the inter-area modes is investigated.

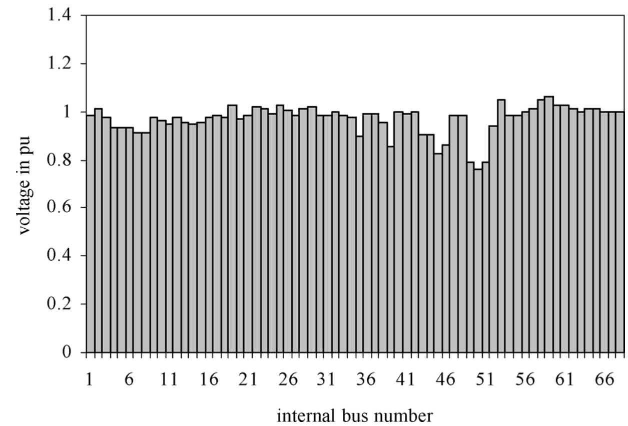

Fig. 7. Bus voltage magnitude profile when the system is heavily stressed in Study System 2.

IV. Selection of Supplementary Input Signals for Damping Inter-Area Oscillations

The input signal to the SVCs used for supplementary control should be responsive to the mode of oscillations to be damped. This can be carried out by using several different input-output controllability analyses such as HSV, RHP-zeros, RGA and MSV. Once the SVC is placed in the system, the choices for the stabilizing signal could be in a wide range of local and global signals. For example, for the SVC placed at bus 101 in the Study System 1, the stabilizing signal could be the magnitude of current, active power, or the reactive power in lines 10-20, 20-3, 3-4, 3-101, 101-13, 13-14, 13-120, and 120-110, and the angular speed of all generators.

To determine the best stabilizing signal, the controllability and observability indices are used through the HSV. A comparison of modal observabilities should be done with care. The modal observability of the line current must not be compared with the modal observability of the line power. For this purpose, signals are categorized in different groups, where each group is made of the same type of signals; for example, magnitude of current with the magnitude of current, power with power, and then the HSV of the different signals in each group is compared. The candidate having larger HSV is more preferable than other candidates. In other words, the candidate having larger HSV contains more information about the system internal states than other candidates. This analysis leaves us with at least four candidates (one for each group) for a further consideration with the RHP-zeros.

A. Study System 1

1) Pre-Fault Condition: For the Study System 1 (see Fig. 1) during the pre-fault condition, the HSV analysis is carried out for the four different groups of the signals (line-current magnitude, active power, reactive power, and the generator angular speed). Among the lines active power (second group), P_{13-14}, P_{20-3}, and P_{13-120} have larger HSV than other line power candidates. The HSVs of these three candidates are shown in Fig. 8. By the definition, the singular values are ordered in descending order, where the first singular value is the largest and others are decreasing monotonically. Table I shows the values of each singular values associated with states (for the first ten states). The

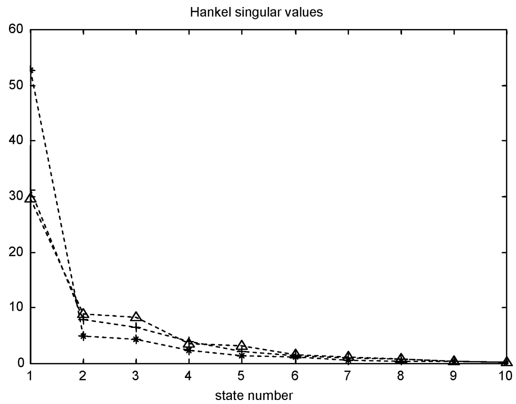

Fig. 8. Study System 1, pre-fault condition. The HSV of selected candidates of the second group: plus-dotted line: P_{20-3}; star-dotted line: P_{13-14}; triangle-dotted line: P_{13-120}.

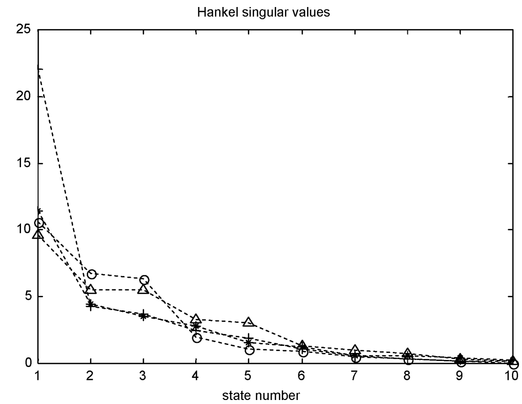

Fig. 9. Study System 1, post-fault condition. The HSV of selected candidates in the second group: plus-dotted line: P_{3-4}; star-dotted line: P_{20-3}; triangle-dotted line: P_{13-120}; circle-dotted line: P_{3-101}.

TABLE I
HANKEL SINGULAR VALUES FOR PRE- AND POST-FAULT CONDITIONS, RELATED TO FIGS. 8 AND 9

The first 10 States	Hankel singular values for Pre-fault condition (Fig. 8)			Hankel singular values for post-fault condition (Fig. 9)			
	P_{20-3}	P_{13-14}	P_{13-120}	P_{3-4}	P_{20-3}	P_{13-120}	P_{3-101}
1	30.94	52.35	29.39	21.87	11.37	9.55	10.50
2	7.95	4.87	8.82	4.28	4.41	5.53	6.78
3	6.60	4.32	8.28	3.72	3.57	5.50	6.36
4	3.95	2.32	3.56	2.43	2.79	3.32	1.99
5	2.14	1.32	3.19	1.92	1.59	3.02	1.06
6	1.47	1.15	1.64	1.06	1.25	1.35	0.94
7	0.918	0.58	1.18	0.544	0.583	1.00	0.46
8	0.831	0.410	0.861	0.306	0.576	0.707	0.301
9	0.437	0.299	0.369	0.171	0.378	0.315	0.134
10	0.264	0.132	0.129	0.154	0.251	0.160	0.040

HSV results for other categories of the signals are as follows: I_{20-3}, I_{10-20}, and $I_{110-120}$ are selected from the first group, $Q_{120-110}$, Q_{10-20}, and Q_{13-120} from the third group and ω of G_4, G_3, and G_1 in the fourth group.

The HSV analysis leaves us with a total of 12 candidates (pre-fault condition) for a further consideration with the RHP-zeros. Table II shows the encountered RHP-zeros for different candidates for the pre-fault condition. It shows that there are four signals not producing RHP-zeros for the pre-fault condition: P_{13-14}, P_{20-3}, P_{13-120}, and $Q_{120-110}$.

2) Post-Fault Condition: The above analyses were carried out for a pre-fault condition. The same procedure will be carried out for a post-fault condition when a three-phase fault occurred at bus 3, and line 3-101 will be disconnected. The selected candidates by the HSV analysis for each group are listed as follows:

The first group: I_{20-3}, I_{3-101}, I_{10-20}, and $I_{110-120}$; the second group: P_{3-4}, P_{20-3}, P_{3-101}, and P_{13-120}; the third group: $Q_{120-110}$, Q_{10-20}, and Q_{13-120}; and the fourth group: ω of G_4, G_3, and G_1. The HSV results for the power group are shown in Fig. 9 and Table I.

The RHP-zeros are calculated for the selected candidates in HSV analysis, and the results are shown in Table II. The table shows that there are only two candidate signals not producing RHP-zeros for both the pre-fault and post-fault conditions, i.e., P_{20-3} and P_{13-120}. Therefore, examining the obtained results

TABLE II
ENCOUNTERED RHP-ZEROS FOR THE STABILIZING SIGNAL CANDIDATES IN STUDY SYSTEM 1

Stabilizing signal candidate	Pre-fault	Post-fault
	RHP-zeros	RHP-zeros
I_{20-3}	$0.055 \pm j2.279$	$1.53 \pm j2.53$
I_{3-101}	-	none
I_{10-20}	8.72×10^{-5}	9.12×10^{-5}
$I_{110-120}$	1.0032×10^{-4}	1.13×10^{-4}
P_{3-4}	-	0.1613
P_{13-14}	none	-
P_{20-3}	none	none
P_{3-101}	-	none
P_{13-120}	**none**	**none**
$Q_{120-110}$	none	0.0036
Q_{10-20}	0.31988	2.0247
Q_{13-120}	3.21×10^{-7}	8.73×10^{-7}
G_4	1.12×10^{-7}	3.47×10^{-7}
G_3	5.23×10^{-9}	8.63×10^{-9}
G_1	7.41×10^{-8}	9.18×10^{-8}

in Table II for both the pre-fault and post-fault conditions, a good choice for the input signal is either P_{20-3} or P_{13-120}. However, based on Figs. 8 and 9, the HSV is better for the signal P_{13-120} than for P_{20-3}, and thus, P_{13-120} is the final choice.

B. Study System 2

The procedure was explained comprehensively for the Study System 1. The same procedure will be applied for the Study System 2 and will be explained briefly in this section. The post-fault condition for the Study System 2 is when a three-phase fault occurred at bus 2, and line 1-2 will be disconnected.

As explained in Section III-B, three SVCs are optimally placed based on modal analysis: the first one at bus 40, the second one at bus 49, and the third one at 50. The choice of stabilizing signal for these three SVCs could be as follows:

SVC at bus 40: I_{40-41}; I_{40-48}; I_{48-47}; I_{41-42}; P_{40-41}; P_{40-48}; P_{48-47}; P_{41-42}.

SVC at bus 49: I_{49-46}; I_{49-52}; I_{46-38}; P_{49-46}; P_{49-52}; P_{46-58}.

SVC at bus 50: I_{50-51}; I_{50-52}; I_{51-45}; P_{50-51}; P_{50-52}; P_{51-45}.

TABLE III
SELECTED CANDIDATE SETS THAT PASSED THE HSV AND RHP-ZERO TESTS IN STUDY SYSTEM 2

NUMBER OF CANDIDATE SETS	CANDIDATE STABILIZING SIGNALS FOR SVCs AT BUS 40, 49 AND 50	Minimum Singular Value	
		Pre-fault	Post-fault
1	I_{40-41}; I_{49-46}; I_{50-51}	-	-
2	I_{40-41}; I_{49-52}; I_{50-51}	-	-
3	I_{40-41}; I_{46-38}; I_{50-51}	1.4310	1.5326
4	I_{40-48}; I_{49-46}; I_{50-51}	-	-
5	I_{40-48}; I_{49-52}; I_{50-51}	-	-
6	I_{40-48}; I_{46-38}; I_{50-51}	4.1529	3.9693
7	I_{48-47}; I_{49-46}; I_{50-51}	-	-
8	I_{48-47}; I_{49-52}; I_{50-51}	-	-
9	I_{48-47}; I_{46-38}; I_{50-51}	1.9890	2.0982
10	I_{41-42}; I_{49-46}; I_{50-51}	-	-
11	I_{41-42}; I_{49-52}; I_{50-51}	-	-
12	I_{41-42}; I_{46-38}; I_{50-51}	-	-
13	I_{48-47}; I_{49-46}; P_{50-51}	-	-
14	I_{40-41}; P_{49-46}; I_{50-51}	-	-
15	I_{40-41}; P_{49-52}; I_{50-51}	-	-
16	I_{40-41}; P_{46-38}; I_{50-51}	-	-
17	I_{40-41}; P_{46-38}; I_{50-52}	-	-
18	I_{40-41}; P_{46-38}; I_{51-45}	-	-
19	I_{40-48}; P_{49-46}; I_{50-51}	-	-
20	I_{40-48}; P_{49-52}; I_{50-51}	-	-
21	I_{40-48}; P_{46-38}; I_{50-51}	-	-
22	I_{48-47}; P_{49-46}; I_{50-51}	-	-
23	I_{48-47}; P_{49-52}; I_{50-51}	-	-
24	I_{48-47}; I_{46-38}; I_{50-51}	-	-
25	I_{48-47}; I_{46-38}; I_{51-451}	-	-
26	I_{41-42}; P_{49-46}; I_{50-51}	-	-
27	I_{41-42}; P_{49-52}; I_{50-51}	-	-
28	I_{41-42}; P_{46-38}; I_{50-51}	-	-
29	I_{40-41}; P_{46-38}; P_{50-51}	-	-
30	I_{40-41}; P_{46-38}; P_{50-52}	-	-
31	I_{40-41}; P_{46-38}; P_{51-45}	-	-
32	P_{40-41}; I_{49-46}; I_{50-51}	-	-
33	P_{40-41}; I_{49-52}; I_{50-51}	-	-
34	P_{40-41}; I_{46-38}; I_{50-51}	2.9999	1.1348
35	P_{40-48}; I_{49-46}; I_{50-51}	-	-
36	P_{40-48}; I_{49-52}; I_{50-51}	-	-
37	P_{40-48}; I_{46-38}; I_{50-51}	**2.4820**	**2.3811**
38	P_{48-47}; I_{49-46}; I_{50-51}	-	-
39	P_{48-47}; I_{49-52}; I_{50-51}	-	-
40	P_{48-47}; I_{46-38}; I_{50-51}	-	0.0801
41	P_{41-42}; I_{49-46}; I_{50-51}	-	-
42	P_{41-42}; I_{49-52}; I_{50-51}	-	-
43	P_{40-41}; P_{49-46}; I_{50-51}	-	-
44	P_{40-41}; P_{49-52}; I_{50-51}	-	-
45	P_{40-41}; P_{46-38}; I_{50-51}	-	-
46	P_{40-41}; P_{46-38}; I_{50-52}	-	-
47	P_{40-41}; P_{46-38}; I_{51-45}	-	-
48	P_{40-48}; P_{49-46}; I_{50-51}	-	-
49	P_{40-48}; P_{49-52}; I_{50-51}	-	-
50	P_{40-48}; P_{46-38}; I_{50-51}	-	-
51	P_{40-48}; P_{46-38}; I_{50-52}	-	-
52	P_{40-48}; P_{46-38}; I_{50-45}	-	-
53	P_{48-47}; P_{49-46}; I_{50-51}	-	-
54	P_{48-47}; P_{49-52}; I_{50-51}	-	-
55	P_{48-47}; I_{46-38}; I_{50-51}	-	-
56	P_{48-47}; I_{46-38}; I_{50-52}	-	-
57	P_{48-47}; I_{46-38}; I_{51-451}	-	-
58	P_{41-42}; P_{49-46}; I_{50-51}	-	-
59	P_{41-42}; P_{49-52}; I_{50-51}	-	-
60	P_{41-42}; P_{46-38}; I_{50-51}	-	-
61	P_{40-41}; P_{46-38}; I_{50-51}	-	-
62	P_{40-41}; P_{46-38}; I_{50-52}	-	-
63	P_{40-41}; P_{46-38}; I_{51-45}	-	-
64	P_{40-48}; P_{46-38}; P_{50-51}	-	-
65	P_{40-48}; P_{46-38}; P_{50-52}	-	-
66	P_{40-48}; P_{46-38}; P_{51-45}	-	-
67	P_{48-47}; P_{46-38}; P_{50-51}	-	-
68	P_{48-47}; P_{46-38}; P_{50-52}	-	-
69	P_{48-47}; P_{46-38}; P_{51-45}	-	-

From the above choice of candidate signals, it is desired to select only one signal for each SVC. For this, there will be 288 possible combinations. To check the HSV for the 288 sets of candidates in an orderly manner, the sets are grouped into eight groups, each group with a combination of current or power signals for each of the three SVCs $(2^3 = 8)$.

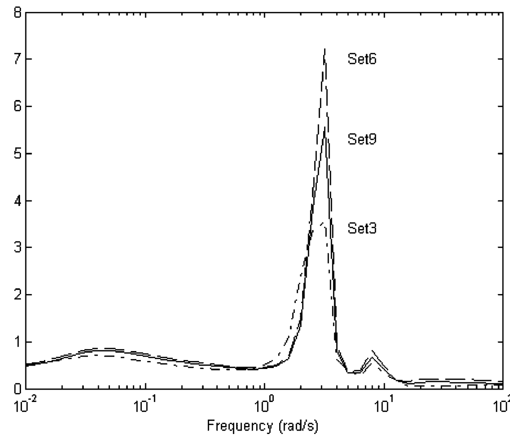

Fig. 10. Study System 2. The RGA-number of candidate sets 3, 6, and 9 (pre-fault).

The 288 sets of candidates are reduced to 69 sets after checking the HSV and RHP-zeros. The results are summarized in Table III. The table lists the 69 sets of candidates, which passed the screening of HSV and RHP-zeros, i.e., they have relatively larger HSV and do not produce RHP-zeros. Since 69 sets are still too many to choose from, additional stability tests are necessary to reduce the number of sets significantly.

For these 69 candidates, the RGA-number is calculated over the frequency spectrum for both pre-fault and post-fault conditions. The six candidate sets, 3, 6, 9, 34, 37, and 40, are first selected since they have relatively smaller RGA-number. The RGA-number of these candidates is shown in Figs. 10–15. Among the six candidate sets, the set 40 is shown to have relatively larger RGA-number compared to the rest of the sets, and thus, the set 40 will be discarded. To demonstrate the difference between the RGA-number of the selected candidates and other candidates, comparisons between the selected set 37 and other sets 31 and 22 are made, which are shown in Figs. 12 and 15, respectively.

The 69 sets of candidates are now reduced to only five sets based on the RGA-number: sets 3, 6, 9, 34, and 37. Five sets are still too many, and one last test is performed, namely, the calculation of MSV. The MSV is calculated for the five sets for both pre-fault and post-fault conditions and tabulated in the last two columns in Table III. As mentioned in Section II-C, it is desirable to have the MSV as large as possible. This condition excludes sets 3 and 34 from the final list because they have relatively smaller MSV in the post-fault condition. Thus, now only three sets are left for the finalist: sets 6, 9, and 37. Among the sets 6 and 9, the candidate set 6 has larger MSV. However, its RGA-numbers are larger compared to the set 9 (see Fig. 10). Therefore, the set 6 is discarded from the three finalists.

Among the two finalists, the RGA-numbers of set 9 are relatively larger compared to the set 37 for pre-fault and post-fault. Therefore, the candidate set 37 is the final choice since it has a better RGA-number while the MSV is relatively large for both

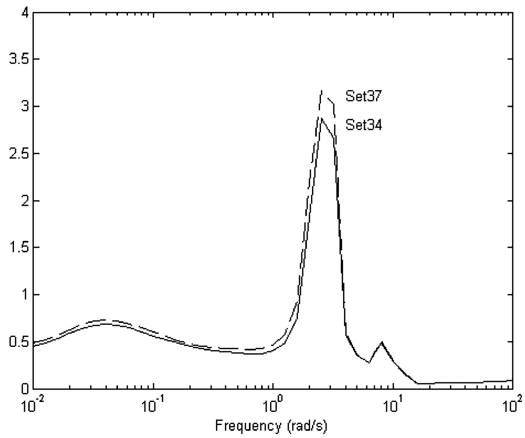

Fig. 11. Study System 2. The RGA-number of candidate sets 34 and 37 (pre-fault).

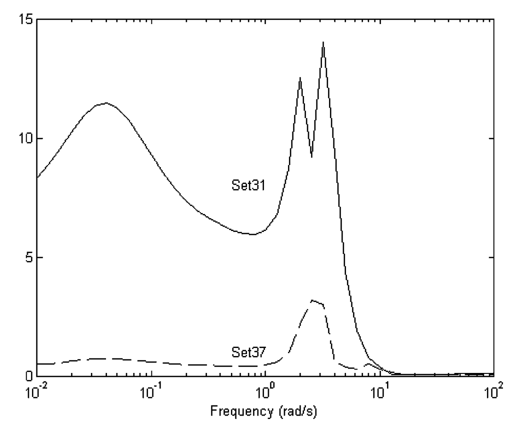

Fig. 12. Study System 2. The RGA-number of candidate sets 31 and 37 (pre-fault).

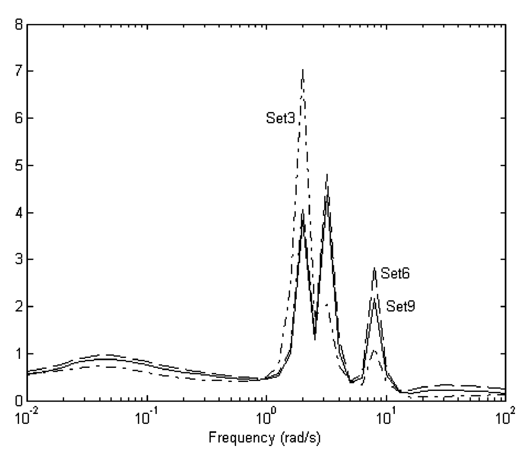

Fig. 13. Study System 2. The RGA-number of candidate sets 3, 6, and 9 (post-fault).

pre- and post-faults. That is, three input signals, P_{40-48}, I_{46-38}, and I_{50-51}, are selected as stabilizing input signals for the SVCs at buses 40, 49, and 50, respectively.

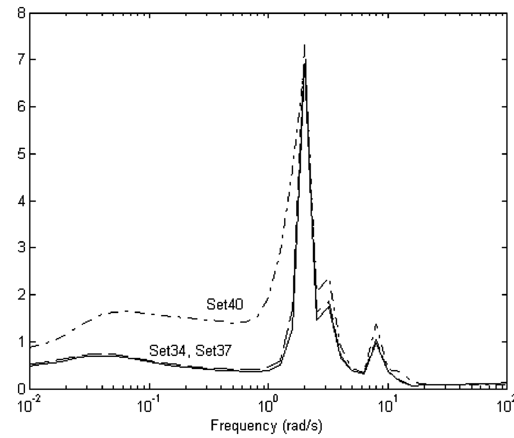

Fig. 14. Study System 2. The RGA-number of candidate sets 34, 37, and 40 (post-fault).

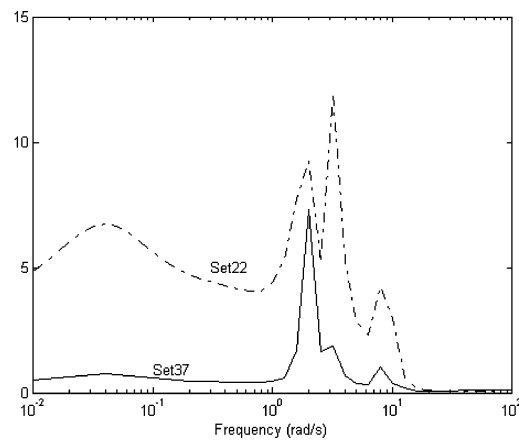

Fig. 15. Study System 2. The RGA-number of candidate sets 37 and 22 (post-fault).

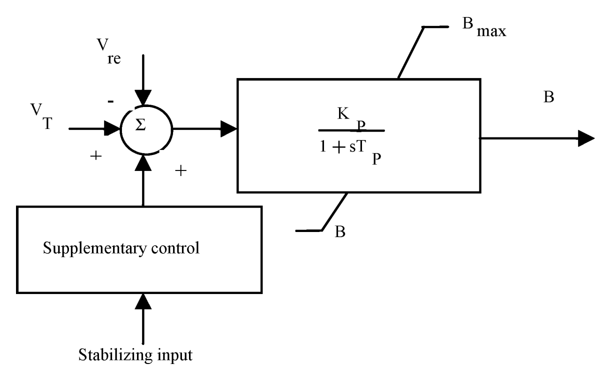

Fig. 16. SVC model with supplementary control.

V. Testing of the Installed SVCs

Fig. 16 shows an SVC model with supplementary control. The installed SVCs with the selected stabilizing input signals are tested in both the frequency and time domain in this section.

A. Frequency-Domain Response

In order to see the effectiveness of the input signal selected, the open-loop transfer function of the SVC with respect to the input signal is plotted in the frequency domain. A high gain at a particular frequency implies that it has a strong effect on

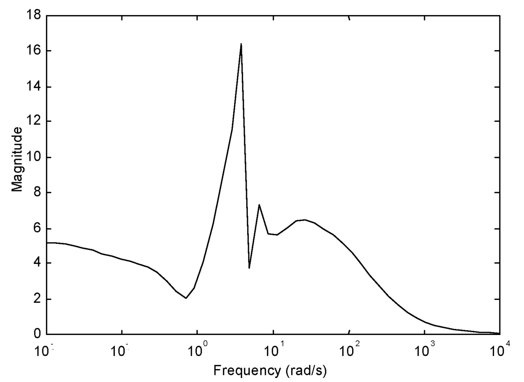

Fig. 17. Study System 1. Open-loop frequency response of the SVC at bus 101 with the input signal P_{13-120}.

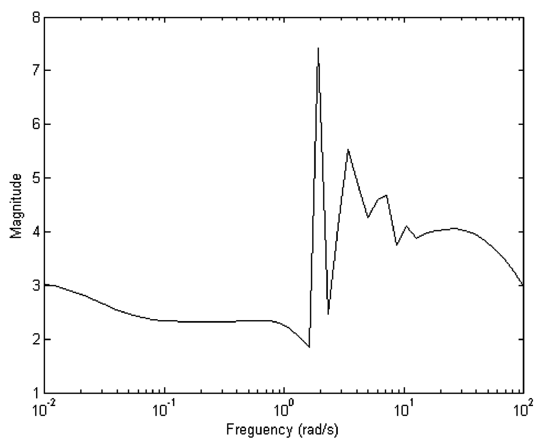

Fig. 18. Study System 2. Open-loop frequency response of the SVC at bus 40 with the input signal P_{40-48}.

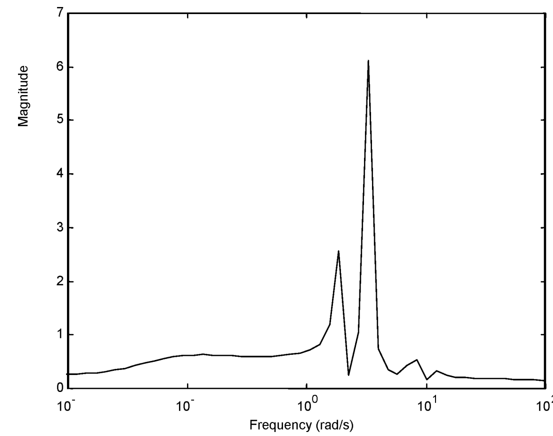

Fig. 19. Study System 2. Open-loop frequency response of the SVC at bus 49 with the input signal I_{46-38}.

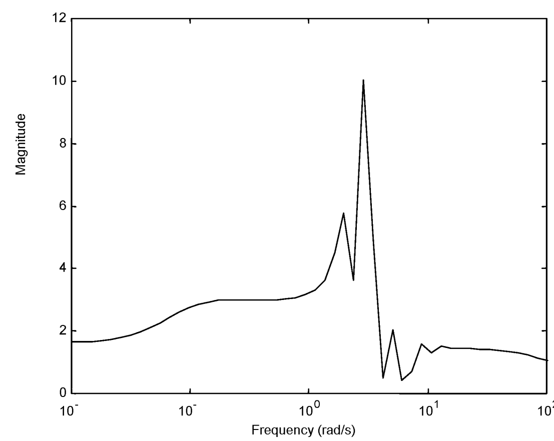

Fig. 20. Study System 2. Open-loop frequency response of the SVC at bus 50 with the input signal I_{50-51}.

damping that particular mode of system oscillation. For the Study System 1, an SVC was placed at bus 101 and the signal P_{13-120}, the line flow between buses 13 and 120, was selected as the stabilizing input signal for the SVC. The stabilizing input signal for the SVC should be responsive to the modes of oscillation to be damped. In order to demonstrate the effectiveness of the located SVC in the two-area power system in controlling the inter-area modes damping, the open-loop frequency responses are shown. Fig. 17 shows the frequency response characteristics of the transfer function between the SVC input and the selected stabilizing input signal (P_{13-120}) shown in Fig. 16. It is very interesting to see that in Fig. 17, the inter-area mode is very dominant in the frequency response due to having a high gain at the frequency of inter-area mode (in the frequency range of 0.1–2 Hz or equality 0.6–12.5 rad/s), which is an indication of good selectivity of the stabilizing input signal. Having higher gain shows that the mode is observable on the output and controllable by the selected stabilizing input signal.

In the Study System 2, three SVCs were placed, one each at buses 40, 49, and 50, and the signals P_{40-48}, I_{46-38}, and I_{50-51}, respectively, were selected as stabilizing input signals for the SVCs. The performance of the SVCs in damping the inter-area oscillation is tested. Figs. 18–20 show the frequency response characteristics of the three transfer function for three different SVCs, which is an indication of good selectivity of the signal for each SVC due to selecting the three different modes in the frequency range of 0.6–12.5 rad/s.

B. Time-Domain Response

To show the effectiveness of the installed SVCs with the selected stabilizing input signal, a time-domain analysis is performed for the Study System 1. Two different signals are selected from Table II for stabilizing signals: a local signal (P_{3-101}) and the global signal (P_{13-120}), and supplementary controllers are designed by H_∞ controller using loop shaping method [25]. Fig. 21 shows the dynamic response of the system following a three-phase fault at bus 3 in the Study System 1 when two different stabilizing input signals are considered. The results show that the global signal selected by the proposed method, P_{13-120}, has a better performance.

For a wide range of signals considered, including local and global signals, it was shown for the Study System 1 that the global signal is selected over the local signals. The global signals can be a remote signal. The use of remote feedback signal is becoming more and more common [27]–[31] and could be a practical reality soon. These signals suffer from the communication delays, but as shown, they may have the strongest observability condition. Therefore, for designing controllers for such

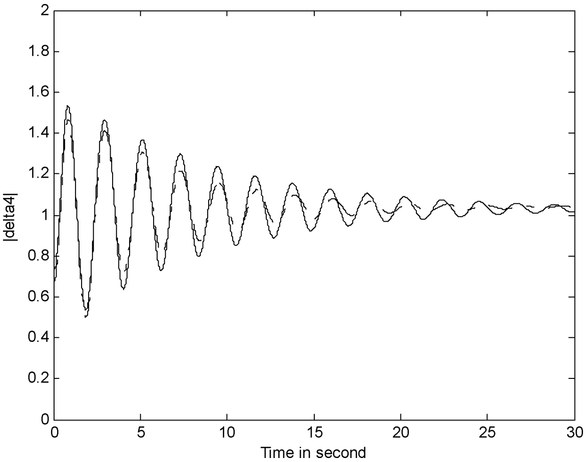

Fig. 21. Dynamic response of the system following a three-phase fault at bus 3 in the Study System 1: dashed line: considering P_{13-120} as stabilizing input signal; solid line: considering P_{3-101} as stabilizing input signal.

system, the communication time delay could be incorporated in the future. When the remote signal is lost, a local signal can be used as a backup signal. Although not optimal, the local signal can have a satisfactory performance as shown in the time-domain response in Fig. 21.

VI. Conclusions

In order to take the advantages of the FACTS devices in the power systems, three SVCs are placed optimally in the Study System 2. For this, the location and size of SVCs are obtained using modal analysis and genetic algorithm. In finding the best locations based on their primary function (voltage stability), both modal analysis and genetic algorithm give the same results. However, the best sizes of SVCs are found only by genetic algorithm. The HSV, RHP-zeros, MSV, and RGA-number are used to select the best supplementary input signal for the SVCs to damp the inter-area oscillations of two study systems. It is concluded that HSV, as an observability and controllability indicator, should be used with care, and the signals compared should be of the same type. The selected candidates from this step are considered for the next step to check for the encountering of the RHP-zeros. The RGA-number is calculated next, and those candidates with smaller RGA-number are selected. The final decision is based on the MSV for the Study System 2. These steps should be done for both the pre-fault and post-fault conditions. The open-loop frequency response of the systems showed the sensitivity of the selected auxiliary signals to the inter-area mode.

References

[1] Y. Mansour, W. Xu, F. Alvarado, and C. Rinzin, "SVC placement using critical modes of voltage instability," *IEEE Trans. Power Syst.*, vol. 9, no. 2, pp. 757–763, May 1994.

[2] L. J. Cai, I. Erlich, and G. Stamtsis, "Optimal choice and allocation of FACTS devices in deregulated electricity market using genetic algorithms," in *Proc. 2005 IEEE Power Eng. Soc. General Meeting*, pp. 201–207.

[3] E. E. El-Araby, N. Yorino, and H. Sasaki, "A comprehensive approach for FACTS devices optimal allocation to mitigate voltage collapse," in *Proc. 2002 IEEE Transmission and Distribution Conf. Exhib.*, pp. 62–67.

[4] Z. Y. Dong, Y. Wang, D. J. Hill, and Y. V. Makarov, "A new approach to power system VAr planning aimed at voltage stability enhancement with feedback control," in *Proc. 1999 Electric Power Engineering. PowerTech Budapest '99*, p. 33.

[5] S. Gerbex, R. Cherkaoui, and A. J. Germond, "Optimal location of multi-type FACTS devices in a power system by means of genetic algorithms," *IEEE Trans. Power Syst.*, vol. 16, no. 3, pp. 537–544, Aug. 2001.

[6] L. Ippolito and P. Siano, "Selection of optimal number and location of thyristor-controlled phase shifters using genetic based algorithms," *Proc. Inst. Elect. Eng., Gen., Transm., Distrib.*, vol. 151, no. 5, pp. 630–637, Sep. 2004.

[7] H. Mori and Y. Goto, "Parallel tabu search based method for determining optimal allocation of FACTS in power systems.," in *Proc. PowerCon on Power System Technology*, 2000, pp. 1077–1082.

[8] S. Gerbex, R. Cherkaoui, and A. J. Germond, "Optimal location of FACTS devices to enhance power system security," in *Proc. 2003 IEEE Bologna PowerTech Conf.*, pp. 23–26.

[9] M. M. Farsangi, Y. H. Song, and K. Y. Lee, "Choice of FACTS device control inputs for damping inter-area oscillations," *IEEE Trans. Power Syst.*, vol. 19, no. 2, pp. 1135–1142, May 2004.

[10] M. M. Farsangi, Y. H. Song, and K. Y. Lee, "On selection of supplementary input signals for STATCOM to damp inter-area oscillations in power systems," in *Proc. 2005 IEEE Power Eng. Soc. General Meeting*, pp. 3068–3073.

[11] E. V. Larsen and J. H. Chow, "SVC control design concepts for system dynamic performance," IEEE Special Publication: Application of Static VAR Systems For System Dynamic Performance, 1987, pp. 53–36.

[12] Q. Zhao and J. Jiang, "Robust SVC controller design for improving power system damping," *IEEE Tran. Energy Convers.*, vol. 10, no. 2, pp. 201–209, Nov. 1995.

[13] Q. Zhao and J. Jiang, "A TCSC damping controller design using robust control theory," *Int. J. Elect. Power Energy Syst.*, vol. 20, no. 1, pp. 25–33, Jan. 1998.

[14] N. Martins and L. T. G. Lima, "Determination of suitable locations for power system stabilizers and static VAR compensators for damping electromechanical oscillations in large scale power systems," *IEEE Trans. Power Syst.*, vol. 5, no. 4, pp. 1455–1469, Nov. 1990.

[15] P. Pourbeik and M. J. Gibbard, "Damping and synchronising torques induced on generators by FACTS stabilizers in multimachine power systems," *IEEE Trans. Power Syst.*, vol. 11, no. 4, pp. 1920–1925, Nov. 1996.

[16] S. E. M. De Oliveira, "Synchronising and damping torque coefficients and power system steady-state stability as affected by static VAR compensators," *IEEE Trans. Power Syst.*, vol. 9, no. 1, pp. 109–119, Feb. 1994.

[17] S. Lee and C. C. Liu, "An output feedback static Var controller for the damping of generator oscillations," *Elect. Power Syst. Res.*, vol. 25, no. 1, pp. 9–16, Feb. 1994.

[18] E. Z. Zhou, "Application of static var compensators to increase power system damping," *IEEE Trans. Power Syst.*, vol. 8, no. 2, pp. 655–661, May 1993.

[19] P. Zhang, A. R. Messina, A. Coonick, and B. J. Cory, "Selection of locations and input signals for multiple SVC damping controllers in large scale power systems," presented at the Proc. 1998 IEEE/Power Eng. Soc. Winter Meeting, Paper IEEE-0-7803-4403-0, pp. 667-670.

[20] A. O. Ekwue, H. B. Wan, D. T. Y. Cheng, and Y. H. Song, "Singular value decomposition method for voltage stability analysis on the National Grid system (NGC)," *Int. J. Elect. Power Energy Syst.*, vol. 21, no. 6, pp. 425–32, 1999.

[21] A. M. A. Hamdan, "An investigation of the significance of singular value decomposition in power system dynamics," *Int. J. Elect. Power Energy Syst.*, vol. 21, no. 6, pp. 417–424, 1999.

[22] P. Kundur, *Power System Stability and Control*. New York: McGraw-Hill, 1994, 1994.

[23] P. Kundur, J. Paserba, V. Ajjarapu, G. Andersson, A. Bose, C. Canizares, N. Hatziargyriou, D. Hill, A. Stankovic, C. Taylor, T. Van Cutsem, and V. Vittal, "Definition and classification of power system stability," *IEEE Trans. Power Syst.*, vol. 19, no. 2, pp. 1387–1401, May 2004.

[24] D. E. Goldberg, *Genetic Algorithms in Search, Optimization, and Machine Learning*. New York: Addison-Wesley, 1989.

[25] S. Skogestad and I. Postethwaite, *Multivariable Feedback Control, Analysis and Design*. New York: Wiley, 1996.

[26] K. Zhou, J. C. Dole, and K. Glover, *Robust and Optimal Control*. Englewood Cliffs, NJ: Prentice-Hall, 1996.

[27] M. E. Aboul-Ela, A. A. Sallam, J. D. McCalley, and A. A. Fouad, "Damping controller design for power system oscillation using global signals," *IEEE Trans. Power Syst.*, vol. 11, no. 2, pp. 767–773, May 1996.
[28] G. M. Taranto and D. M. Falcao, "Robust decentralised control design using genetic algorithms in power system damping control," *Proc. Inst. Elect. Eng., Gen., Transm., Distrib.*, vol. 145, no. 1, pp. 1–6, Jan. 1998.
[29] C. S. de Araujo and J. C. de Castro , "Partially decentralized controller for damping interarea oscillations in power systems," in *Proc. Amer. Control Conf.*, 1998, vol. 6, pp. 3415–3419.
[30] H. Chen and Z. Guo, "LMI-based wide-area robust damping control," in *Proc. IEEE/Power Eng. Soc. Transmission and Distribution Conf. Exhib.*, 2005, pp. 1–6.
[31] B. Chaudhuri and B. C. Pal, "Robust damping of multiple swing modes employing global stabilizing signals with a TCSC," *IEEE Trans. Power Syst.*, vol. 19, no. 1, pp. 499–506, Feb. 2004.

Malihe M. Farsangi received the B.S. degree in electrical engineering from Ferdousi University, Mashhad, Iran, in 1995 and the Ph.D. degree in electrical engineering from Brunel Institute of Power Systems, Brunel University, London, U.K., in 2003.

Since 2003, she has been with Kerman University, Kerman, Iran, where she is currently an Assistant Professor of electrical engineering. Her interests include power system control, stability, FACTS, and intelligent system applications.

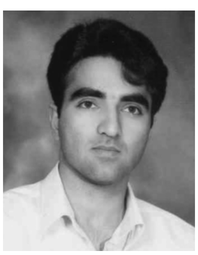

Hossein Nezamabadi-pour received the B.S. degree in electrical engineering from Kerman University, Kerman, Iran, in 1998 and the M.Sc. and Ph.D. degrees in electrical engineering from Tarbait Modarres University, Tehran, Iran, in 2000 and 2004, respectively.

Since 2004, he has been with Kerman University, where he is currently an Assistant Professor of electrical engineering. His interests include pattern recognition, soft computing, evolutionary computation, and image processing.

Yong-Hua Song (SM'93) is a Professor of electrical engineering and Pro-Vice-Chancellor at the University of Liverpool, Liverpool, U.K. He began his academic career as a Postdoctoral Research Fellow at Tsinghua University, Beijing, China, in 1989 and subsequently held posts in the U.K. at Bristol, Bath, and Liverpool John Moores Universities. In 1997, he joined Brunel University, London, U.K., as Royal Academy of Engineering/British Energy/BNFL/Siemens Research Professor of Power Systems. He was Pro-Vice-Chancellor with responsibility for Graduate Studies from 2004 to 2006.

Dr. Song was awarded a D.Sc. in 2001 for his significant contributions to power system research and knowledge, by Brunel University. He is a Fellow of the Royal Academy of Engineering and of the IEE.

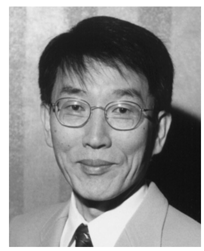

Kwang Y. Lee (F'01) received the B.S. degree in electrical engineering from Seoul National University, Seoul, Korea, in 1964, the M.S. degree in electrical engineering from North Dakota State University, Fargo, in 1968, and the Ph.D. degree in system science from Michigan State University, East Lansing, in 1971.

He has been with Michigan State University, Oregon State University, University of Houston, and the Pennsylvania State University and Baylor University, where he is currently a Professor and Chair of the Electrical and Computer Engineering Department and Director of Power Systems Control Laboratory. His interests include power system control, operation, planning, and intelligent system applications to power systems.

Dr. Lee is an Associate Editor of IEEE TRANSACTIONS ON NEURAL NETWORKS and Editor of IEEE TRANSACTIONS ON ENERGY CONVERSION. He is also a registered Professional Engineer.